COMMUNICATION

Supercapacitors

ADVANCED
ENERGY
MATERIALS

www.advenergymat.de

Design and Performance of Rechargeable Sodium Ion Batteries, and Symmetrical Li-Ion Batteries with Supercapacitor-Like Power Density Based upon Polyoxovanadates

Jia-Jia Chen, Jian-Chuan Ye, Xia-Guang Zhang, Mark D. Symes, Shao-Cong Fan, De-Liang Long, Ming-Sen Zheng, De-Yin Wu, Leroy Cronin,* and Quan-Feng Dong*

The polyanion $Li_7V_{15}O_{36}(CO_3)$ is a nanosized molecular cluster ($\approx$1 nm in size), that has the potential to form an open host framework with a higher surface-to-bulk ratio than conventional transition metal oxide electrode materials. Herein, practical rechargeable Na-ion batteries and symmetric Li-ion batteries are demonstrated based on the polyoxovanadate $Li_7V_{15}O_{36}(CO_3)$. The vanadium centers in $\{V_{15}O_{36}(CO_3)\}$ do not all have the same $V^{IV/V}$ redox potentials, which permits symmetric devices to be created from this material that exhibit battery-like energy density and supercapacitor-like power density. An ultrahigh specific power of 51.5 kW kg^{-1} at 100 A g^{-1} and a specific energy of 125 W h kg^{-1} can be achieved, along with a long cycling life (>500 cycles). Moreover, electrochemical and theoretical studies reveal that $\{V_{15}O_{36}(CO_3)\}$ also allows the transport of large cations, like Na^+, and that it can serve as the cathode material for rechargeable Na-ion batteries with a high specific capacity of 240 mA h g^{-1} and a specific energy of 390 W h kg^{-1} for the full Na-ion battery. Finally, the polyoxometalate material from these electrochemical energy storage devices can be easily extracted from spent electrodes by simple treatment with water, providing a potential route to recycling of the redox active material.

The quest for high-performance, low-cost energy storage systems has boosted interest in new materials for rechargeable Li-ion and Na-ion batteries and supercapacitors. A key goal is to improve the energy and power densities of these devices by improving the kinetics of the processes occurring at the electrode/electrolyte interface.[1] In Li-ion batteries, the insertion of Li^+ into bulk electrode materials can provide high capacity density (around 250 mA h g^{-1}),[1a] but the insertion of Li^+ is diffusion-controlled and so such processes tend to be slow in the limited interstitial space of transition metal oxides. Supercapacitors store energy electrostatically through the formation of electrical double layers at the electrode/electrolyte interface, and thus enable good performance at high rates (but with low energy density, usually lower than 50 W h kg^{-1}).[2] Hence, it would be interesting to design a single electrochemical energy storage device which combines battery-like energy density with a supercapacitor-like rate performance.[3] Indeed, this has motivated numerous studies of Li-ion supercapacitors, nanohybrid capacitors and asymmetric supercapacitors, as well as a variety of hybrid materials.[4] For example, some transition metal oxides and sulfides used in Li-ion batteries can also be used for supercapacitors. However, although some such materials (e.g., $LiFePO_4$) can undergo lithiation/delithiation without changes in volume, most transition metal oxides suffer from drastic volume changes during multielectron redox reactions at the high current densities characteristic of rechargeable batteries or supercapacitors.[5]

Concerns have also been raised regarding the likely future availability of Li and hence its future cost, especially in light of the projected orders-of-magnitude increase in Li usage for batteries in electric vehicles and smart grids.[6] This need to reduce Li loadings has in turn led to research into Na-ion batteries as alternatives to Li-ion batteries due to the lower cost of Na and its greater natural abundance.[7] However, the conventional host metal-oxide lattices commonly explored for Li-ion batteries are

Dr. J.-J. Chen, Dr. J.-C. Ye, Dr. X.-G. Zhang, S.-C. Fan, Prof. M.-S. Zheng, Prof. D.-Y. Wu, Prof. L. Cronin, Prof. Q.-F. Dong
State Key Laboratory of Physical Chemistry of Solid Surfaces
Department of Chemistry
College of Chemistry and Chemical Engineering
iChem (Collaborative Innovation Center of Chemistry for Energy Materials)
Xiamen University
Xiamen, Fujian 361005, China
E-mail: Lee.Cronin@glasgow.ac.uk; qfdong@xmu.edu.cn
Dr. J.-J. Chen, Dr. M. D. Symes, Dr. D.-L. Long, Prof. L. Cronin
WestCHEM
School of Chemistry
the University of Glasgow
University Avenue
Glasgow G12 8QQ, UK

close-packed oxide-ion arrays connected by first-row transition metals, and lack the interstitial space for rapid Na$^+$ diffusion. This is due to the much larger ionic radius of Na$^+$ (1.02 Å) compared to Li$^+$ (0.76 Å).[8] Although layered-oxide structures, such as Na$_x$[Fe$_{1/2}$Mn$_{1/2}$]O$_2$,[9] are thought to be promising candidates with high capacities (up to 190 mA h g^{-1}), they still suffer from poor Na$^+$ transport kinetics. A three-phase separation mechanism has been found among the Li$_4$Ti$_5$O$_{12}$ family of electrodes for Li-/Na-ion batteries; nevertheless, the rate performances are still low due to the slow transport kinetics of Na$^+$ ions.[10] Compared to recent progress in the development of anode materials for Na-ion batteries,[11] it is still a big challenge to find suitable cathode materials with specific capacities >200 mA h g^{-1}.[12]

Various strategies have been developed to solve the problems mentioned above for rechargeable batteries and supercapacitors, such as employing nanosized materials. Many electrode materials for batteries show higher rates performance at the nanoscale, and nanosize materials also exhibit much higher capacitances for supercapacitors, due to the increased specific surface area and better access to redox reaction sites. Moreover, the mobility of larger cations (like Na$^+$) can be greatly enhanced in nanostructured metal oxide electrode materials, thus increasing the rate performance of the resulting Na-ion batteries. It is, therefore, intriguing to consider the effects of reducing the length scales of the materials used in these electrodes down to the molecular scale. At such dimensions, it might prove possible to combine very high power densities with very high energy densities in a single device. Polyoxometalates are promising candidates for this, due to their nanoscale polyanion molecular structure and varied redox properties, which present a range of interesting electrochemical phenomena,[13] including for use as the cathode material in Li-ion batteries.[14] Polyoxometalates can be considered to be "electron sponges," able to undergo reversible multielectron reactions with high structural stability.[15] In our previous work,[14] we found that Li ions exhibit different kinetic behavior in Li$_7$[V$_{15}$O$_{36}$(CO$_3$)] when compared to traditional bulk vanadium oxides, with greater mobility of the Li ions allowing excellent rates performance to be achieved. Moreover, nanosize clusters such as these ($\approx$1–5 nm in size)[16] and the open host frameworks that they produce can deliver a higher surface:bulk ratio than conventional transition metal oxides, and hence facilitate the uptake/removal and transport of large cations.[17] Thus by adjusting the molecular structure of polyoxometalates, they have the potential to exhibit different electrochemical behaviors to suit the demands of various electrochemical applications.

Herein, we exploit the fact that the vanadium centers in the Li$_7$V$_{15}$O$_{36}$(CO$_3$) polyanion do not all have the same redox potentials, in order to use {V$_{15}$O$_{36}$(CO$_3$)} as the active material in both the cathode and the anode in symmetrical Li-ion batteries. These devices combine battery-like energy densities (125 W h kg^{-1}) with supercapacitor-like power densities (51.5 kW kg^{-1}), due to the unique structure of {V$_{15}$O$_{36}$(CO$_3$)} compared to conventional metal oxides. These devices show robustness to cycling (>500 cycles) and ultrafast rate performance up to 100 A g^{-1}. Moreover, electrochemical studies and density functional theory (DFT) calculations reveal that {V$_{15}$O$_{36}$(CO$_3$)} also allows the transport of large cations, like Na$^+$, and that it can store a large number of cations and thus
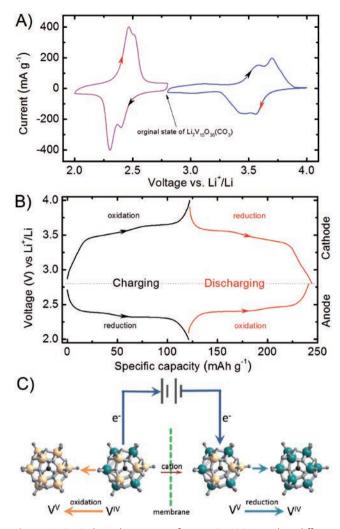

Figure 1. A) Cyclic voltammetry of Li$_7$[V$_{15}$O$_{36}$(CO$_3$)] within different voltage ranges at a scan rate of 0.2 mV s^{-1}, B) half-cell charge–discharge curves at a current density of 100 mA g^{-1}, C) a simple model to demonstrate the charging process of symmetric electrochemical devices based on {V$_{15}$O$_{36}$(CO$_3$)}. V^V centers are shown in yellow and V^{IV} centers in teal. The reverse process corresponds to the discharging process.

serve as the cathode material for rechargeable Na-ion batteries with a high specific capacity of 240 mA h g^{-1} and an energy density of 390 W h kg^{-1} for the full Na-ion battery.

{V$_{15}$O$_{36}$(CO$_3$)} is a mixed-valence polyoxometalate that formally contains eight V^{IV} centers and seven V^V centers. X-ray photoelectron spectroscopy results (Figures S1 and S2, Supporting Information) provide evidence for this: the initial state of the {V$_{15}$O$_{36}$(CO$_3$)} electrode displays two V 2p$_{3/2}$ peaks (at 516.9 and 518.1 eV), which correspond to vanadium in oxidation states V^{4+} and V^{5+}.[18] These two types of V center have different redox potentials. Thus, when the counter ion is Li$^+$, {V$_{15}$O$_{36}$(CO$_3$)} shows two different sets of redox potentials with high reversibility at 3.5 and 2.4 V versus Li$^+$/Li (**Figure 1**A), corresponding to the two different V environments. As shown in Figure 1B, both the V^{IV} and the V^V centers in {V$_{15}$O$_{36}$(CO$_3$)} exhibit a specific capacity of around 120 mA h g^{-1} for Li$^+$ storage at their respective voltage ranges.

**ADVANCED
SCIENCE NEWS**
www.advancedsciencenews.com
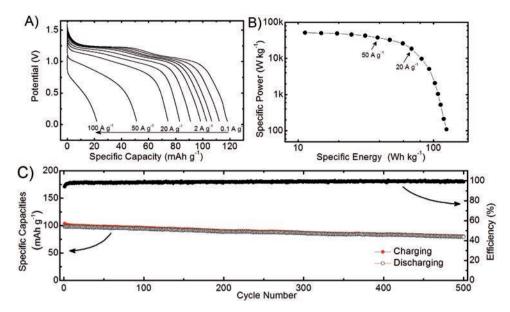
**ADVANCED
ENERGY
MATERIALS**
www.advenergymat.de

Figure 2. The electrochemical performance of a symmetric $Li_7[V_{15}O_{36}(CO_3)]$ device A) discharge curves at 0.1, 0.2, 0.5, 1, 2, 5, 10, 20, 50, and 100 A g^{-1}, respectively, B) specific power versus specific energy, C) long cycling performance at 1 A g^{-1}.

This suggests that the development of an electrochemical energy storage device with $\{V_{15}O_{36}(CO_3)\}$ on both the positive and negative electrodes should be possible, due to the different valence states of V that are possible in this molecule. As illustrated in Figure 1C, during the charging process of this kind of symmetric device, the seven V^{IV} centers in $\{V_{15}O_{36}(CO_3)\}$ are electrochemically oxidized, releasing Li^+ and electrons on the positive side. This also causes a shift of the V $2p_{3/2}$ peak to a higher binding energy, indicating that the V^{IV} centers in the positive electrode are oxidized to V^V. The electrons then travel through the external circuit to reduce the seven V^V centers on the negative side, with concomitant influx of Li^+, which thus also results in a shift of V $2p_{3/2}$ peak to a lower binding energy (indicative of reduction from V^V to V^{IV}) in the negative electrode (Figures S1 and S2, Supporting Information). Hence, during the reversible discharging process, the V^V centers in $\{V_{15}O_{36}(CO_3)\}$ on the positive electrode are electrochemically reduced and the V^{IV} centers on the negative electrode are re-oxidized to V^V, thus releasing the energy stored in the device.

On account of the multielectron storage ability and fast redox kinetics of $\{V_{15}O_{36}(CO_3)\}$, this symmetric device should have the ability to exhibit supercapacitor-like rate performance with a high energy density. As shown in **Figure 2**A, at a current density of 0.1 A g^{-1}, it shows a specific capacity of 120 mA h g^{-1} with a voltage plateau at 1.2 V. This is typical battery-like behavior and is distinct from the linear drop-off in voltage-versus-time curves characteristic of conventional supercapacitors. The specific energy is high (up to 125 W h kg^{-1}), much higher than that hitherto reported for polyoxometalate-based supercapacitors and other Li-ion supercapacitors (the method to calculate the energy density is given in Figure S3 in the Supporting Information).[19] Moreover, this symmetric device also shows ultrafast rate performance with low polarization at high charge–discharge current densities. When the current densities

are increased from 0.1 to 2 A g^{-1}, there is no obvious polarization of the voltage plateau while the specific capacity decreases from 120 to 98 mA h g^{-1} (see Figures S4 and S5 in the Supporting Information). Even over the high current density range from 5 to 20 A g^{-1}, it still delivers high specific capacities from 91 to 75 mA h g^{-1}. This result confirms that this device can be charged up to 75% of its maximum specific capacity within 66 s and still exhibit a high specific power of 5.2 kW kg^{-1} at a current density of 5 A g^{-1}. Furthermore, it can even show a 62.5% specific capacity retention after a charging time of 13 s at the higher current density 30 A g^{-1} with a specific power of 18.5 kW kg^{-1} (Figure 2B). Moreover, an ultrahigh specific power of 51.5 kW kg^{-1} can still be obtained after less than 1 s charging time at an ultrahigh current density of 100 A g^{-1}. Considering the volumetric density of $Li_7[V_{15}O_{36}(CO_3)]$ to be 2.15 g cm^{-3}, this symmetric device shows a high volumetric energy density of 270 Wh L^{-1} and a volumetric power density of 110 kW L^{-1}. Meanwhile, it also exhibits excellent cycling performance at a high current density of 1 A g^{-1}. The storage capability of this symmetric device is also very stable at a low current density of 100 mA g^{-1} over 50 cycles. Hence, this device shows an initial capacity of 120 mA h g^{-1} with capacity retention of 95% after 50 cycles (Figure S6, Supporting Information). Moreover, as shown in Figure 2C, Coulombic efficiencies during the fast charge–discharge processes are almost 100% over a longer cycling of 500 cycles. The specific capacity after 500 cycles is still 82 mA h g^{-1} which means that there is only 0.03% degradation per cycle. As also confirmed by the field-emission scanning electron microscopy images (SEM) of $Li_7[V_{15}O_{36}(CO_3)]$ at the charged and discharged states, the morphologies of the electrodes are not obviously different when compared to the starting state of $Li_7[V_{15}O_{36}(CO_3)]$ (Figures S7 and S8, Supporting Information). Thus, the $Li_7[V_{15}O_{36}(CO_3)]$ symmetric device can exhibit highly stable performance during a long cycling test. As a result, this battery based on $\{V_{15}O_{36}(CO_3)\}$
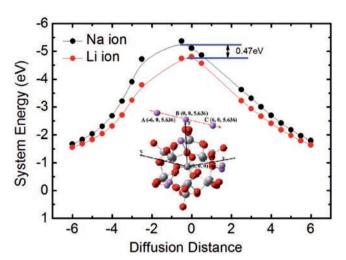
Figure 3. DFT calculations of the transfer energy barrier of Li$^+$ and Na$^+$ during the migration versus cation diffusion distance in $\{V_{15}O_{36}(CO_3)\}$. The inset picture shows the migration model for Li$^+$ and Na$^+$ cations in $\{V_{15}O_{36}(CO_3)\}$. The coordinate of the carbon atom in CO_3^{2-} was defined as a coordinate origin (0, 0, 0).

exhibits a supercapacitor-like power density with battery-like energy density and stable cycling ability.

In addition to the application of $\{V_{15}O_{36}(CO_3)\}$ in a symmetrical Li-ion battery, it can also be used as a high capacity cathode for Na-ion batteries. According to the theoretical study summarized in **Figure 3**, when diffusing to the surface of $\{V_{15}O_{36}(CO_3)\}$ clusters, Li$^+$ has a lower energy barrier than Na$^+$ on account of the smaller radius of Li$^+$. Meanwhile, the DFT calculations suggest that the transfer energy barrier of Li$^+$ and Na$^+$ is only slightly different (around 0.47 eV), which is close to the theoretical potential difference of Li and Na (around 0.33 eV). This difference suggests that the diffusion of a larger cation in the structure of $\{V_{15}O_{36}(CO_3)\}$ is still feasible, in turn suggesting that viable Na-ion batteries could be obtained using this material.

The DFT calculation results are also consistent with the AC impedance investigation of the Na$^+$ diffusion coefficient. The diffusion coefficient of Na$^+$ (2.83×10^{-12} cm^2 s^{-1}, Figures S10, S11 and Table S3, Supporting Information) in $\{V_{15}O_{36}(CO_3)\}$ is even higher than the Li$^+$ diffusion coefficient in pure LiFePO$_4$-type materials ($\approx 10^{-15}$ cm^2 s^{-1}) and exceeds that of many recently reported P2-structure Na-ion cathode materials.[20] Unlike the sluggish Na$^+$ movement that occurs in conventional host metal-oxides for Na-ion batteries, the kinetics of the reversible redox processes in $\{V_{15}O_{36}(CO_3)\}$ are much faster, thus suggesting excellent Na$^+$ storage metrics for $\{V_{15}O_{36}(CO_3)\}$.

As shown in **Figure 4**A, $\{V_{15}O_{36}(CO_3)\}$ shows two distinct and reversible plateaus within the voltage window 3.8–1.2 V versus Na$^+$/Na, evincing similar potential behavior to that for other recently reported cathode materials for Na-ion batteries.[21] A reversible specific capacity of around 240 mA h g^{-1} can be obtained at a current density of 50 mA g^{-1}, with a specific capacity of 100 mA h g^{-1} during the first charge (Figure S12, Supporting Information). The change in valence of the V centers in $\{V_{15}O_{36}(CO_3)\}$ during cycling when used as the cathode material in a Na-ion battery also follows
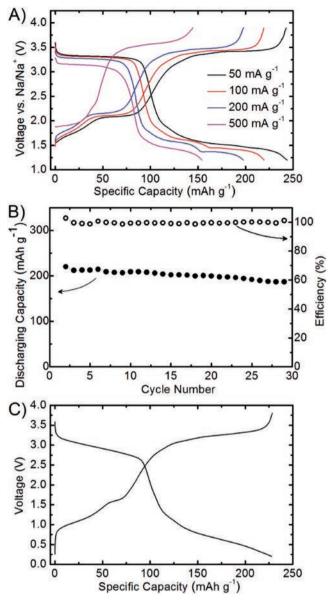

Figure 4. A) The discharge–charge curves of a half-cell of Li$_7$[V$_{15}$O$_{36}$(CO$_3$)] with metallic Na as the anode at different current densities, B) cycling performance of Li$_7$[V$_{15}$O$_{36}$(CO$_3$)] as the cathode for a rechargeable Na-ion battery at 100 mA g^{-1}, C) the charge–discharge curve of a prototype full battery using Li$_7$[V$_{15}$O$_{36}$(CO$_3$)] as the cathode and Kureha hard carbon as the anode at a current density of 25 mA g^{-1}.

a similar trend to that in the discussion above for the symmetric Li-ion device (see Figure S13 in the Supporting Information). Li$_7$[V$_{15}$O$_{36}$(CO$_3$)] also displays excellent rate performance and retains reversible discharge capacities of between 240 and 155 mA h g^{-1} at a range of current densities from 50 to 500 mA g^{-1} (Figure 4A). Moreover, $\{V_{15}O_{36}(CO_3)\}$ also delivers stable cycling performance: it can retain a stable and reversible capacity of 190 mA h g^{-1} at 100 mA g^{-1} after 30 cycles (Figure 4B). This is also consistent with SEM images of $\{V_{15}O_{36}(CO_3)\}$ in Na-ion battery electrodes in the charged and discharged states (Figure S14, Supporting Information): the morphologies are almost the same in both cases. Our results

show that Na$^+$ can diffuse easily within $\{V_{15}O_{36}(CO_3)\}$ and can be taken up/removed reversibly during these multielectron redox reactions. When coupled with a hard carbon to give a fully rechargeable Na-ion battery (Kureha carbon, Figure 4C and Figure S15), a reversible capacity of 230 mA h g^{-1} was obtained over the voltage range $0.2 \leq V \leq 3.8$ V (on the basis of the mass of $\{V_{15}O_{36}(CO_3)\}$). As a result, such Na-ion batteries show a higher specific energy (390 W h kg^{-1}) than other reported full Na-ion batteries,[22] and are comparable even with commercially available Li-ion battery cathodes such as LiMn$_2$O$_4$ ($\approx$450 W h kg^{-1}). This results confirms that $\{V_{15}O_{36}(CO_3)\}$ is a very promising candidate for use in the production of Na-ion batteries.

Last but not least, unlike other bulk metal oxides used in rechargeable batteries, polyoxometalates are typically water-soluble, which could afford a ready route to recovery of the metals from batteries at the end of their useful lives. In order to demonstrate the recovery of the redox active material from used batteries, we sonicated discharged-state cathodes (that had been cycled ten times) in water, to extract the polyoxometalates into solution (see Table S4 in the Supporting Information). Inductively coupled plasma optical emission spectrometry (ICP-OES) results confirmed that concentration of these extracts gave residues with a mass that corresponded to around 80% of that used in the production of the electrodes. This result confirms that the active material can be easily recovered after battery cycling.

In conclusion, we have demonstrated a symmetric Li-ion battery with a battery-like energy density and supercapacitor-like power density, which uses the polyoxovanadate $\{V_{15}O_{36}(CO_3)\}$ on both electrodes. On account of the multielectron redox chemistry and fast cation diffusion within this material, this electrochemical energy storage device exhibits an excellent rate performance with a high specific power of 51.5 kW kg^{-1} (volumetric power density of 110 kW L^{-1}), as well as a considerable specific energy of 125 W h kg^{-1} (volumetric energy density of 270 W h L^{-1}). This type of symmetric device is both straightforward to fabricate and inherently safe, due to the nonflammable nature of metal oxides. Moreover, we show that $\{V_{15}O_{36}(CO_3)\}$ can also act as a high capacity cathode in a Na-ion battery configuration with good performance. Finally, we have shown that it is feasible to recover the active material from cycled electrodes. Considering the very varied nature of polyoxometalates and the ability to tailor their redox properties, we believe that these materials will find numerous applications in batteries and supercapacitors.

Supporting Information

Supporting Information is available from the Wiley Online Library or from the author.

Acknowledgements

Conflict of Interest

The authors declare no conflict of interest.

Keywords

[1] a) J. M. Tarascon, M. Armand, *Nature* **2001**, *414*, 359; b) D. Aurbach, *J. Power Sources* **2000**, *89*, 206.

[2] C. Zhong, Y. Deng, W. Hu, J. Qiao, L. Zhang, J. Zhang, *Chem. Soc. Rev.* **2015**, *44*, 7484.

[3] H. Zhang, X. Yu, P. V. Braun, *Nat. Nanotechnol.* **2011**, *6*, 277.

[4] a) K. Naoi, W. Naoi, S. Aoyagi, J.-i. Miyamoto, T. Kamino, *Acc. Chem. Res.* **2013**, *46*, 1075; b) A. S. Arico, P. Bruce, B. Scrosati, J.-M. Tarascon, W. van Schalkwijk, *Nat. Mater.* **2005**, *4*, 366.

[5] M. S. Islam, C. A. J. Fisher, *Chem. Soc. Rev.* **2014**, *43*, 185.

[6] V. Etacheri, R. Marom, R. Elazari, G. Salitra, D. Aurbach, *Energy Environ. Sci.* **2011**, *4*, 3243.

[7] M. D. Slater, D. Kim, E. Lee, C. S. Johnson, *Adv. Funct. Mater.* **2013**, *23*, 947.

[8] N. Yabuuchi, K. Kubota, M. Dahbi, S. Komaba, *Chem. Rev.* **2014**, *114*, 11636.

[9] N. Yabuuchi, M. Kajiyama, J. Iwatate, H. Nishikawa, S. Hitomi, R. Okuyama, R. Usui, Y. Yamada, S. Komaba, *Nat. Mater.* **2012**, *11*, 512.

[10] Y. Sun, L. Zhao, H. Pan, X. Lu, L. Gu, Y.-S. Hu, H. Li, M. Armand, Y. Ikuhara, L. Chen, X. Huang, *Nat. Commun.* **2013**, *4*, 1870.

[11] a) H. Pan, X. Lu, X. Yu, Y.-S. Hu, H. Li, X.-Q. Yang, L. Chen, *Adv. Energy Mater.* **2013**, *3*, 1186; b) K. Tang, L. Fu, R. J. White, L. Yu, M.-M. Titirici, M. Antonietti, J. Maier, *Adv. Energy Mater.* **2012**, *2*, 873; c) W. Li, S.-L. Chou, J.-Z. Wang, J. H. Kim, H.-K. Liu, S.-X. Dou, *Adv. Mater.* **2014**, *26*, 4037; d) X. Xie, T. Makaryan, M. Zhao, K. L. Van Aken, Y. Gogotsi, G. Wang, *Adv. Energy Mater.* **2016**, *6*, 1502161; e) N. Zhang, X. Han, Y. Liu, X. Hu, Q. Zhao, J. Chen, *Adv. Energy Mater.* **2015**, *5*, 1401123.

[12] a) Y. Jiang, Z. Yang, W. Li, L. Zeng, F. Pan, M. Wang, X. Wei, G. Hu, L. Gu, Y. Yu, *Adv. Energy Mater.* **2015**, *5*, 1402104; b) S. Xu, Y. Wang, L. Ben, Y. Lyu, N. Song, Z. Yang, Y. Li, L. Mu, H.-T. Yang, L. Gu, Y.-S. Hu, H. Li, Z.-H. Cheng, L. Chen, X. Huang, *Adv. Energy Mater.* **2015**, *5*, 1501156; c) Y. Dong, S. Li, K. Zhao, C. Han, W. Chen, B. Wang, L. Wang, B. Xu, Q. Wei, L. Zhang, X. Xu, L. Mai, *Energy Environ. Sci.* **2015**, *8*, 1267; d) J. Zhang, H. Wen, L. Yue, J. Chai, J. Ma, P. Hu, G. Ding, Q. Wang, Z. Liu, G. Cui, L. Chen, *SMALL* **2017**, *13*, 1601530.

[13] a) C. Busche, L. Vila-Nadal, J. Yan, H. N. Miras, D.-L. Long, V. P. Georgiev, A. Asenov, R. H. Pedersen, N. Gadegaard, M. M. Mirza, D. J. Paul, J. M. Poblet, L. Cronin, *Nature* **2014**, *515*, 545; b) B. Rausch, M. D. Symes, G. Chisholm, L. Cronin, *Science* **2014**, *345*, 1326; c) M. D. Symes, L. Cronin, *Nat. Chem.* **2013**, *5*, 403.

[14] J.-J. Chen, M. D. Symes, S.-C. Fan, M.-S. Zheng, H. N. Miras, Q.-F. Dong, L. Cronin, *Adv. Mater.* **2015**, *27*, 4649.

[15] a) H. Wang, S. Hamanaka, Y. Nishimoto, S. Irle, T. Yokoyama, H. Yoshikawa, K. Awaga, *J. Am. Chem. Soc.* **2012**, *134*, 4918; b) Y. Nishimoto, D. Yokogawa, H. Yoshikawa, K. Awaga, S. Irle, *J. Am. Chem. Soc.* **2014**, *136*, 9042.

[16] D.-L. Long, E. Burkholder, L. Cronin, *Chem. Soc. Rev.* **2007**, *36*, 105.

[17] R. Kawahara, S. Uchida, N. Mizuno, *Chem. Mater.* **2015**, *27*, 2092.

[18] G. Silversmit, D. Depla, H. Poelman, G. B. Marin, R. De Gryse, *J. Electron Spectrosc. Relat. Phenom.* **2004**, *135*, 167.

[19] a) H.-Y. Chen, G. Wee, R. Al-Oweini, J. Friedl, K. S. Tan, Y. Wang, C. L. Wong, U. Kortz, U. Stimming, M. Srinivasan, *ChemPhysChem* **2014**, *15*, 2162; b) A.K. Cuentas-Gallegos, M. Lira-Cantú, N. Casañ-Pastor, P. Gómez-Romero, *Adv. Funct. Mater.* **2005**, *15*, 1125; c) M. Yang, B. G. Choi, S. C. Jung, Y.-K. Han, Y. S. Huh, S. B. Lee, *Adv. Funct. Mater.* **2014**, *24*, 7301; d) J. Suarez-Guevara,

V. Ruiz, P. Gomez-Romero, *J. Mater. Chem. A* **2014**, *2*, 1014; e) X. Han, P. Han, J. Yao, S. Zhang, X. Cao, J. Xiong, J. Zhang, G. Cui, *Electrochim. Acta.* **2016**, *196*, 603.

[20] a) Y. Zhu, C. Wang, *J. Phys. Chem. C* **2010**, *114*, 2830; b) S. Guo, Y. Sun, J. Yi, K. Zhu, P. Liu, Y. Zhu, G.-z. Zhu, M. Chen, M. Ishida, H. Zhou, *NPG Asia Mater.* **2016**, *8*, e284; c) N. A. Katcho, J. Carrasco, D. Saurel, E. Gonzalo, M. Han, F. Aguesse, T. Rojo, *Adv. Energy Mater.* **2017**, *7*, 1601477; d) Z.-Y. Li, R. Gao, L. Sun, Z. Hu, X. Liu, *J. Mater. Chem. A* **2015**, *3*, 16272.

[21] a) E. Talaie, V. Duffort, H. L. Smith, B. Fultz, L. F. Nazar, *Energy Environ. Sci.* **2015**, *8*, 2512; b) R. J. Clement, J. Billaud, A. R. Armstrong, G. Singh, T. Rojo, P. G. Bruce, C. P. Grey, *Energy Environ. Sci.* **2016**, *9*, 3240.

[22] a) J. Song, L. Wang, Y. Lu, J. Liu, B. Guo, P. Xiao, J.-J. Lee, X.-Q. Yang, G. Henkelman, J. B. Goodenough, *J. Am. Chem. Soc.* **2015**, *137*, 2658; b) S. Guo, H. Yu, P. Liu, Y. Ren, T. Zhang, M. Chen, M. Ishida, H. Zhou, *Energy Environ. Sci.* **2015**, *8*, 1237.